Syndiotactic Polystyrene Physical Gels: Guest Influence on Structural Order in Molecular Complex Domains and Gel Transparency

Christophe Daniel,* Antonio Avallone, and Gaetano Guerra

Dipartimento di Chimica, Università di Salerno, Via Ponte don Melillo, 84084 Fisciano (SA), Italy

Received May 19, 2006; Revised Manuscript Received August 16, 2006

ABSTRACT: Correlation lengths of crystalline domains of syndiotactic polystyrene (sPS) gels prepared in different solvents, and those of derived aerogels, have been investigated by wide-angle X-ray diffraction. The correlation length (D_{010}), along the direction perpendicular to the *ac* layers of close-packed enantiomorphous s(2/1)2 helices, is strongly dependent on the chemical nature of the guest molecules not only for molecular complex phases of gels but also for the nanoporous crystalline δ phase of aerogels. Moreover, for a large series of solvents, it has been clearly established that sPS gel transparency is markedly dependent on the solvent and regularly increased as D_{010} correlation length is decreased.

Introduction

Syndiotactic polystyrene (sPS) presents a complex polymorphic behavior,[1] which can be described in terms of two crystalline forms with trans-planar chains (α and β[2]) and two crystalline forms with **s**(2/1)2 helical chains (γ and δ[3]). Moreover, this polymer in its helical conformation forms crystalline molecular complexes (clathrate[4] and intercalate[5]) with several different low-molecular-mass compounds.

In several organic solvents, sPS can form thermoreversible gels where the polymer rich-junctions are formed by crystalline domains. Depending on solvent-type and/or thermal history, two kinds of gel can be obtained: past-like opaque gels for which the crystalline domains present the trans-planar β crystalline phase[6] and elastic gels[7,8] for which the crystalline domains present s(2/1)2 helical molecular complex (clathrate[7] or intercalate[8]) phases.

Independent of the crystalline structure of the junction zones of the sPS gels, high porosity aerogels can be easily obtained by supercritical CO_2 extraction procedures.[9] These aerogels present crystalline phase (β or δ) and crystalline texture (lamellae or fibrils), which are determined by the crystalline phase (β or molecular-complex, respectively) of the junction zones of the starting sPS physical gels.

Helical sPS gels are generally more stable than trans-planar sPS gels. In fact, for instance, rheological measurements have shown that the dynamic storage modulus G', for equal polymer concentrations, is generally higher for gels with helical crystalline phases than for gels with trans-planar crystalline phases.[6b] Hence, helical sPS gels can be also prepared with very dilute solutions (polymer concentration as low as 1 wt %).

Several literature studies report that helical sPS gels can be either translucent (in benzene,[7b] toluene,[7e] carbon tetrachloride,[7b] or chloroform[7b]) or turbid (in decahydronaphthalene,[7e] or *o*-xylene[7d]).

In this communication, the transparency of helical sPS gels with several different solvents has been quantitatively compared. Moreover, these gel transparency data have been rationalized by quantitative information on correlation lengths of crystalline domains (molecular complex phases for gels and δ phases for the corresponding aerogels), which has been achieved by wide-angle X-ray diffraction measurements.

Experimental Section

The syndiotactic polystyrene used in this study was manufactured by Dow Chemicals under the trademark Questra 101. ^{13}C nuclear magnetic resonance characterization showed that the content of syndiotactic triads was over 97%.The mass average molar mass obtained by gel permeation chromotography (GPC) in trichlorobenzene at 135 °C was found to be $M_w = 3.2 \times 10^5$ g mol^{-1} with a polydispersity index $M_w/M_n = 3.9$. Solvents were purchased from Aldrich and used without further purification.

All sPS gel samples were prepared in hermetically sealed test tubes by heating the mixtures above the boiling point of the solvent until complete dissolution of the polymer and the appearance of a transparent and homogeneous solution had occurred. Then the hot solution was cooled to room temperature where gelation occurred.

Aerogel samples were obtained by treating native gels with a SFX 200 supercritical carbon dioxide extractor (ISCO Inc.) using the following conditions: $T = 45$ °C; $P = 200$ bar; extraction time $t = 60$ min.

X-rays diffraction patterns were obtained on a Bruker D8 automatic diffractometer operating with nickel-filtered Cu Kα radiation.

Evaluation of the correlation length D of the crystalline domains (where an ordered disposition of the atoms is maintained) was effected using the Scherrer formula

$$D = 0.9\lambda/(\beta \cos \theta)$$

where β is the full width at half-maximum expressed in radiant units, λ is the wavelength and θ the diffraction angle. For $\beta < 1°$, the value of β was corrected from the experimental effects applying the procedure described in ref 10. In particular, a KBr powder sample having a full width at half-maximum, under the same geometrical conditions, of 0.17° was used.

The β values were determined directly from peak intensities after subtraction of the amorphous signal from the X-ray diffraction patterns (see Supporting Information for further information on the determination method of the correlation lengths).

Light transmission measurements were carried out with a Perkin-Elmer Lambda EZ201 UV/vis spectrometer. Gel samples were directly prepared in quartz cells of 1 mm thickness.

Scanning electron micrographs were obtained using an ASSING LEO scanning electron microscope.

* Corresponding author. E-mail: cdaniel@unisa.it.

10.1021/ma061124k CCC: $33.50
Published on Web 09/27/2006

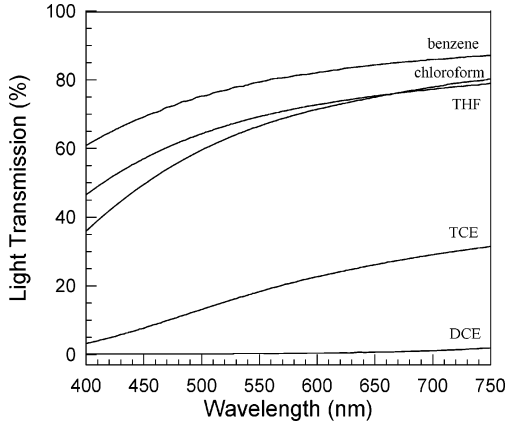

Figure 1. Visible light transmission for sPS gels (thickness 1.0 mm) prepared in benzene, chloroform, tetrahydrofuran (THF), trichloroethylene (TCE), and 1,2-dichloroethane (DCE) at $C_{pol} = 0.10$ g/g.

Results and Discussion

Transmission curves in the visible wavelength range of sPS gels, having a thickness of 1.0 mm and prepared at $C_{pol} = 10$ wt % in benzene, chloroform, tetrahydrofuran (THF), trichloroethylene (TCE), and 1,2-dichloroethane (DCE) are reported in Figure 1. These transmission curves greatly differ depending on the solvent: for instance, the gel prepared with DCE is totally opaque while the gel prepared in benzene is transparent.

The light transmittance calculated by integration of the transmission curves in the range 400−750 nm are listed in column 2 of Table 1.

In general, the gel turbidity or opacity can originate from the size of the polymer-rich domains and from the difference in refractive index between the solvent and the polymer-rich phase.

The sPS gel polymer-rich domains can be easily observed, after solvent extraction procedures by a supercritical fluid leading to the corresponding aerogels. In fact, these procedures generally allow to avoid the collapse of the gel structure and thus preserve the morphology of polymer-rich phase of the native gel.[9,13]

Results show that all sPS aerogels obtained from gels of Table 1 present a similar fibrillar morphology. This is shown, for instance, in Figure 2 by the scanning electron micrographs of aerogels obtained by supercritical CO_2 extraction from gel prepared in THF, chloroform, DCE, and TCE at $C_{pol} = 0.1$ g/g, showing for all the aerogels fibril diameters in the range 20−110 nm.

It is worth emphasizing that differences observed in gel light transmittances cannot be explained by differences in fibril diameters. In particular aerogels obtained from gels prepared in TCE (Figure 2d) present similar fibril diameters ($\phi = 50 \pm 13$ nm) than aerogels obtained from gels prepared in THF (Figure 2a, $\phi = 50 \pm 13$ nm) and chloroform (Figure 2b, $\phi = 46 \pm 13$ nm) while the light transmittance values of the corresponding gels are totally different. It is also worth adding that small differences observed in sample micrographs reported in Figure 2 such as fibril bundles (Figure 2a) cannot either explain the different gel light transmittance values. Indeed, the bundle distribution is not homogeneous and depending on the region shown on the micrograph, bundles can be present or not (see Supporting Information).

Thus, we can conclude that differences observed in gel light transmittances cannot be explained by the occurrence of different morphology or size of the polymer-rich domains.

It is worth noting that similar fiber range diameter has also been observed with scanning electron microscopy for sPS/naphthalene (40−95 nm)[14a] and sPS/chloroform (20−100 nm)[14b] gels after freeze-drying.

The observed differences in gel light transmittance cannot be either explained by differences in refractive index between the solvent and the polymer-rich phase. For instance, DCE and chloroform or *p*-xylene and *m*-xylene have practically the same refractive index (see column 3 of Table 1) while gels prepared in these couples of solvents display totally different light transmittance.

We have explored, by X-ray diffraction measurements, the possibility that the different transparency of sPS gels could be related to the structural order in the crystalline junctions of the gels. In our analysis, particular attention has been devoted to the (010) reflection, corresponding to the *ac* planes, which (not only for the δ phase[3] but also for all known sPS molecular complex phases, both clathrate[4] and intercalate[5]) are formed by the close packing of enantiomorphous s(2/1)2 helices (see, e.g., Figure 1 in ref 15a). In fact, a recent study on structural order in sPS cast films has shown that the chemical nature of the guest can have a strong influence on the correlation length perpendicular to these (010) planes and a weak influence on the correlation length along other crystalline directions.[12] It is also worth adding that these *ac* planes present the highest planar density and hence correspond to the generally preferred uniplanar orientation[15] and present the lowest permeability to guest molecules.[16]

Typical X-ray diffraction patterns in the 2θ range 4−12° of gels prepared in THF, benzene, *p*-xylene, and DCE at $C_{pol} = 0.20$ g/g are reported in Figure 3.

Since the amount of crystallites is small and the X-ray solvent absorption is important, the quality of the diffraction patterns is poor and well-resolved Bragg peaks are not always displayed. Moreover, the (010) reflection, which is strong for the empty δ phase, can be very weak for some molecular complex phases.[4,5] In particular, for the gels prepared in THF, benzene and *p*-xylene we can clearly observe the diffraction peak of (010) planes at 2θ (Cu Kα) = 7.80°, $2\theta = 5.95°$, and $2\theta = 7.90°$ while this diffraction peak is barely present for the gel prepared in DCE and it is not detected for the gel prepared in chloroform (diffraction pattern not shown here). The position of the diffraction peaks for gels obtained in THF, DCE and *p*-xylene are indicative of clathrate phases[4b,4d,7j] while the low angle diffraction peak observed at $2\theta = 5.95°$ with benzene is characteristic of an intercalate phase.[5,8] From the diffraction patterns of Figure 3, the dimensions of crystallites can be evaluated with accuracy only for gels prepared in benzene, THF and *p*-xylene and the correlation length perpendicular to (010) planes (i.e., *ac* planes) D_{010} is equal to 4.5, 6.3, and 15.2 nm, respectively.

A much more accurate evaluation of the correlation lengths D can be achieved for aerogels obtained by supercritical CO_2 extraction of the solvent present in the native gels. Typical X-ray diffraction patterns, after subtraction of the amorphous halo (see Supporting Information), of aerogels obtained from gels prepared in benzene, THF, TCE and DCE at $C_{pol} = 0.10$ g/g are reported in Figure 4.

The presence of strong reflections located at 2θ (Cu Kα) = 8.3° (010), 13.5° ($(\bar{1}11)$ and (101)), 16.8° (111), 20.7° ($(\bar{3}21)$ and (301)), 23.5° ($\bar{4}11$) and the absence of a strong diffraction peak at $2\theta \cong 10.6°$ ($\bar{2}10$) indicates that, in agreement with a previous report,[9] the crystalline phase of aerogels is the

Table 1. Light Transmittance Values of SPS Gels in Different Solvents, Solvent Physical Properties (Refractive Index, Molecular Volume, and Solubility Parameter) and Correlation Lengths of the Crystalline Domains, D_{010} and $D_{\bar{4}11}$, of Aerogel Samples Obtained by Supercritical CO_2 Extraction of Gels[d]

solvent	LT[a] (%)	n_D^{20}	MV[b] (nm^3)	SP[c] δ ($Mpa^{1/2}$)	$D_{\bar{4}11}$ (nm) aerogel	D_{010} (nm) aerogel	D_{010}(nm) film[12]
benzene	79	1.501	0.148	18.8[11a]	6.9	4.6	4.0
1,3,5-trimethylbenzene	79	1.499	0.231	18.0[11a]	6.4	5.1	
o-dichlorobenzene	73	1.551	0.187	20.5[11a]	6.3	6.1	
m-xylene	69	1.497	0.203	18.2[11b]		7.0	5.9
chloroform	69	1.445	0.133	19[11a]	8.4	7.5	5.3
tetrahydrofuran (THF)	66	1.407	0.135	18.6[11a]	7.3	6.9	5.2
toluene	59	1.496	0.177	18.2[11a]	7.2	8.8	–
trichloroethylene (TCE)	19	1.476	0.149	18.8[11a]	6.3	11.5	7.2
p-xylene	21	1.495	0.204	18[11a]	6.7	14.5	7.7
1,2-dichloroethane (DCE)	0.6	1.444	0.131	20[11a]	6.0	15.4	14.0

[a] Light transmittance evaluated by integration of the light transmission curves in the range 400−750 nm obtained for sPS gels having a thickness of 1 mm. [b] Molecular volume evaluated from molar mass (M) and density (ρ) through $MV = M/\rho N_A$. [c] Solubility parameter. [d] For the sake of comparison D_{010} values measured for solution cast films (data by Daniel et al.[12]) are reported in the last column.

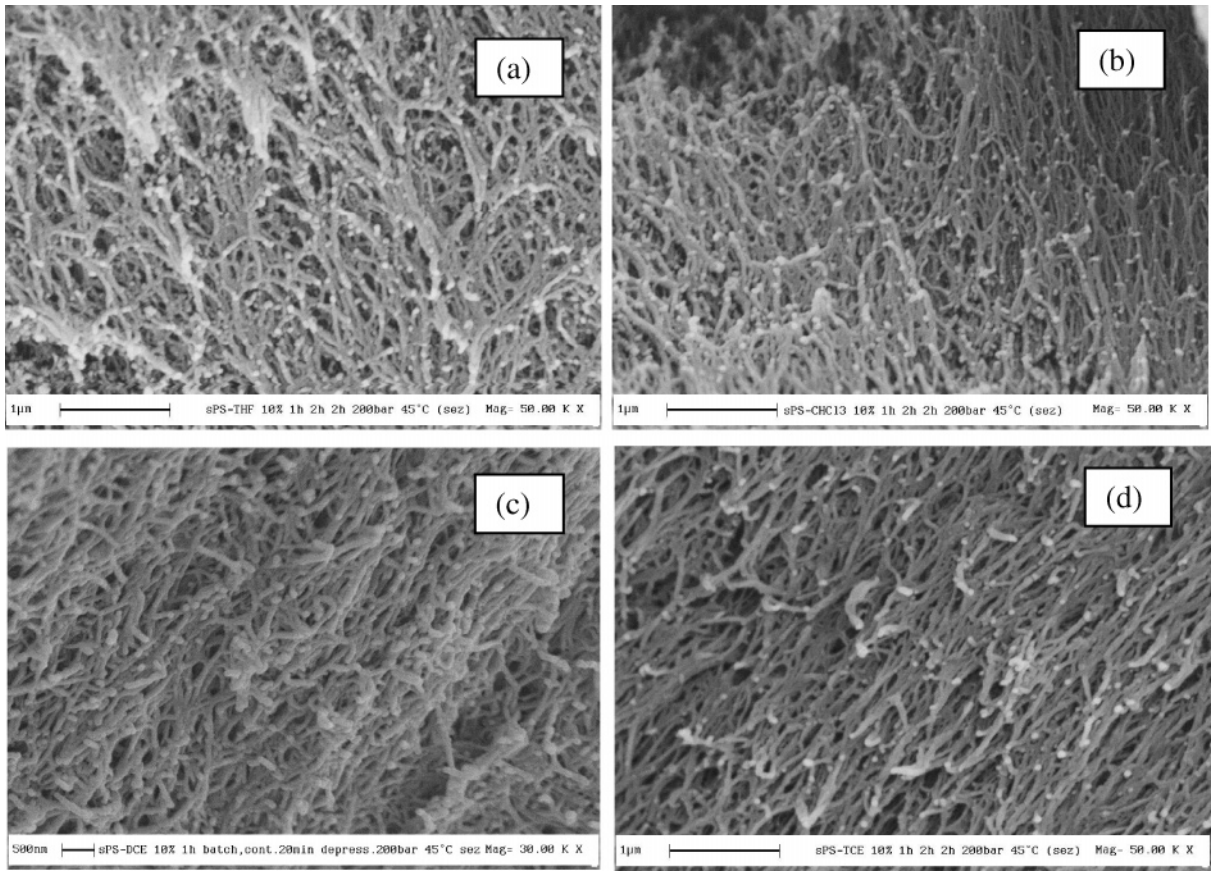

Figure 2. Scanning electron micrographs of aerogels obtained from gels prepared at $C_{pol} = 0.10$ g/g in THF (a), chloroform (b), DCE (c), and TCE (d). Magnification ×50000 for all micrographs but *c* (×30000); scale as indicated.

nanoporous δ-phase[3a] independent of the solvent used to form the gel.

A closer look to the diffraction patterns reported in Figure 4 shows that most diffraction peaks are broad and their widths are nearly independent of the solvent used to form the native gel, as observed for instance for the rather isolated ($\bar{4}11$) diffraction peak (located at $2\theta_{Cu\ K\alpha} = 23.5°$). However, the (010) diffraction peak (located at $2\theta_{Cu\ K\alpha} = 8.3°$) can be broad or narrow depending on the solvent used to form the native gel. For instance, it is narrow for aerogels prepared from TCE and DCE gels, indicating a high structural order along the direction perpendicular to (010) planes (i.e., *ac* planes). This phenomenon is more clearly shown in Table 1 where the correlation lengths of the ($\bar{4}11$) and (010) diffraction peak evaluated for all the examined aerogels are reported in columns 6 and 7, respectively.

It is also worth noting that for aerogels obtained from gels prepared in benzene, THF and *p*-xylene the values of D_{010} are 4.6, 6.9, and 14.5 nm, i.e., similar to D_{010} values determined for the native gels (4.5, 6.3, and 15.2 nm; see comments to Figure 2). Hence, the structural order initially formed in gels is essentially maintained after solvent extraction by supercritical CO_2, leading to the corresponding aerogels.

For the sake of comparison with the D_{010} values measured for aerogels, last column of Table 1 presents the D_{010} values measured for molecular complex crystalline phases of films cast from polymer solutions,[12] in the same solvents used for gel preparation. The comparison indicates that correlation length perpendicular to (010) planes presents a similar guest dependence for both crystallization technique (film casting or gel formation). Hence, the present results well agree with the

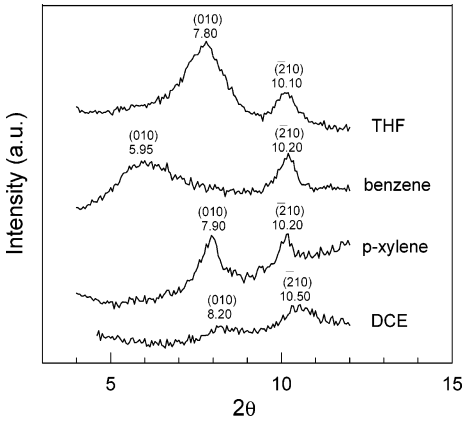

Figure 3. X-ray diffraction patterns in the 2θ range $4-12°$ for gels prepared in THF, benzene, *p*-xylene, and DCE at $C_{pol} = 0.20$ g/g. The diffraction peaks have been indexed by comparison with the diffraction patterns of the known crystalline structure of sPS molecular complexes.[1d,g-h]

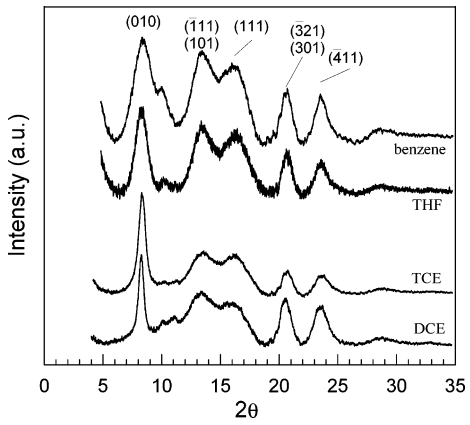

Figure 4. X-ray diffraction patterns of aerogels obtained from gels prepared in benzene, THF, TCE, and DCE at $C_{pol} = 0.10$ g/g (the amorphous signal has been subtracted for all the spectra).

previous hypothesis that the correlation length perpendicular to the (010) planes of the different sPS molecular complex phases is essentially determined by the strength of the occurring host−guest interactions.[12] In this respect, it is worth adding that no correlation occurs between D_{010} and the Bragg distances (d_{010})[12] neither with the guest molecular volume (fourth column of Table 1) nor with the solubility parameter (fifth column of Table 1).

In Figure 5, the gel light transmittance data (second column of Table 1) are reported vs the correlation length perpendicular to the *ac* planes (D_{010}, seventh column of Table 1).

We can clearly observe that the gel light transmittance regularly decreases with increasing the structural order along the direction perpendicular to (010) planes. A higher gel turbidity is often associated with the formation of larger size crystal domains. In this respect, it worth emphasizing that the correlation length D_{010} depends not only on crystalline order but also on the size of crystal domains along the direction perpendicular to the (010) planes.

Finally, it is also worth adding that the correlation between gel light transmittance and the structural order holds both for gels with an intercalate phase (benzene and 1,3,5-trimethylbenzene) or with a clathrate phase (all the other guests of Table 1).

Conclusions

In this paper, sPS physical gels presenting molecular-complex crystalline phases with several different solvents, as well as the corresponding aerogels, have been characterized by wide-angle X-ray diffraction. In particular, the correlation lengths (i.e., the distance for which the structural order is maintained) along different crystal directions have been evaluated, from width at half-maximum of the main diffraction peaks.

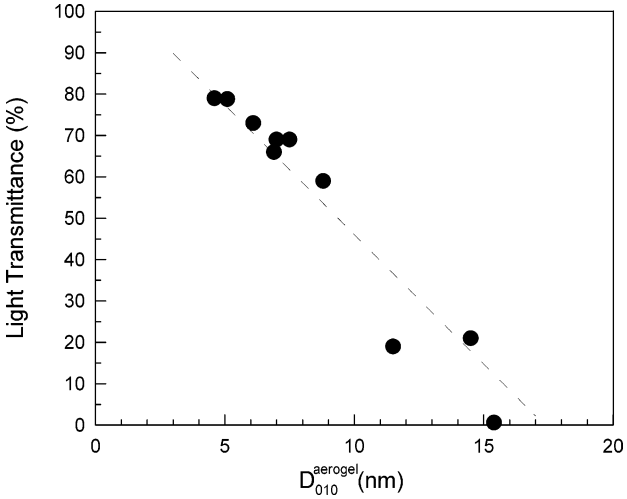

Figure 5. Variation of the gel light transmittance vs the correlation length of (010) planes $D_{010}^{aerogel}$($C_{pol} = 10$ wt %, thickness = 1.0 mm).

The chemical nature of the guest has a strong influence on the correlation length perpendicular to the (010) planes, i.e., the crystalline planes presenting the highest planar density, due to the close packing of enantiomorphous s(2/1)2 helices. This correlation length, $D_{010,}$ can change depending on the guest from ca. 4.5 to 15.5 nm, while the guest influence for correlation length along other crystalline directions is generally poor.

The guest influence on D_{010} values observed for the crystalline phases of gels and aerogels is similar to that one observed for solution cast films. This confirms the previous hypothesis that D_{010} mainly increases with the strength of host−guest interactions into sPS molecular complex phases.[12]

The paper also presents quantitative evaluations of the large differences in light transmission between sPS gels presenting molecular-complex crystalline phases with different solvents. Moreover, the large guest dependence of the sPS gel transparency has been rationalized on the basis of the observed differences in structural order along the direction perpendicular to the (010) planes. In fact, the gel light transmittance does not depend on the solvent refractive index or morphology of the polymer-rich domains (always fibrillar) but regularly decreases with increasing correlation length D_{010} (Table 1 and Figure 5).

Acknowledgment. Financial support of the "Ministero dell'Istruzione, dell'Università e della Ricerca" (Prin 2004) and of Regione Campania (Legge 5 and Centro di Competenza) is gratefully acknowledged. The authors are also greatly indebted to Stefano Cardea for the SEM micrographs and to Davide Alfano for experimental support and useful discussions.

Supporting Information Available: Text giving information concerning the fibril bundle distribution and the method used to determine the correlation lengths, including figures showing the X-ray diffraction patterns of aerogels and SEM micrographs. This material is available free of charge via the Internet at http://pubs.acs.org.

References and Notes

(1) (a) Guerra, G.; Vitagliano, V. M.; De Rosa, C.; Petraccone, V.; Corradini, P. *Macromolecules* **1990**, *23*, 1539−1544. (b) Chatani, Y.;

Shimane, Y.; Inoue, Y.; Inagaki, T.; Ishioka, T.; Iijtsu, T.; Yukimori, T. *Polymer* **1992**, *33*, 488−492.
(2) (a) De Rosa, C.; Rapacciuolo, M.; Guerra, G.; Petraccone, V.; Corradini, P. *Polymer* **1992**, *33*, 1423−1428. (b) Chatani, Y.; Shimane, Y.; Ijitsu, T.; Yukinari, T. *Polymer* **1993**, *34*, 1625−1629.
(3) (a) De Rosa, C.; Guerra, G.; Petraccone, V.; Pirozzi, B. *Macromolecules* **1997**, *30*, 4147−4152. (b) Milano, G.; Venditto, V.; Guerra, G.; Cavallo, L.; Ciambelli, P.; Sannino, D. *Chem. Mater.* **2001**, *13*, 1506−1511.
(4) (a) Immirzi, A.; de Candia, F.; Iannelli, P.; Zambelli, A.; Vittoria, V.; *Makromol. Chem., Rapid Commun.* **1988**, *9*, 761−764. (b) Chatani, Y.; Shimane, Y.; Inagaki, T.; Iijtsu, T.; Yukimori, T.; Shikuma, H. *Polymer* **1993**, *34*, 1620−1624. (c) Chatani, Y.; Inagaki, T.; Shimane, Y.; Shikuma, H. *Polymer* **1993**, *34*, 4841−4845. (d) De Rosa, C.; Rizzo, P.; Ruiz de Ballesteros, O.; Petraccone, V.; Guerra, G. *Polymer* **1999**, *40*, 2103−2110. (e) Tarallo, O.; Petraccone, V. *Macromol. Chem. Phys.* **2004**, *205*, 1351−1360. (f) Tarallo, O.; Petraccone, V. *Macromol. Chem. Phys.* **2005**, *206*, 672−679.
(5) (a) Petraccone, V.; Tarallo, O.; Venditto, V.; Guerra, G. *Macromolecules* **2005**, *38*, 6965−6971. (b) Tarallo, O.; Petraccone, V.; Venditto, V.; Guerra, G. *Polymer* **2006**, *47*, 2402−2410.
(6) (a) Li, Y.; Xue, G. *Macromol. Rapid Commun.* **1998**, *19*, 549−552. (b) Daniel, C.; Alfano, D.; Guerra, G.; Musto, P. *Macromolecules* **2003**, *36*, 1713−1716.
(7) (a) Kobayashi, M.; Nakaoki, T.; Ishihara, N. *Macromolecules* **1990**, *23*, 78−83. (b) Kobayashi, M.; Kosaza, T. *Appl. Spectrosc.* **1993**, *9*, 1417−1424. (c) Deberdt, F.; Berghmans, H. *Polymer* **1993**, *34*, 2192−2201. (d) Deberdt, F.; Berghmans, H. *Polymer* **1994**, *35*, 1694−1704. (e) Daniel, C.; Dammer, C.; Guenet, J. M. *Polymer* **1994**, *35*, 4243−4246. (f) Kobayashi, M.; Yoshioka, T.; Kozasa, T.; Tashiro, K.; Suzuki, J.-I.; Funahashi, S.; Izumi, Y. *Macromolecules* **1994**, *27*, 1349−1354. (g) Kobayashi, M.; Yoshioka, T.; Imai, M.; Itoh, Y. *Macromolecules* **1995**, *28*, 7376−7385. (h) Roels, T.; Deberdt, F.; Berghmans, H. *Prog. Colloid Polym. Sci.* **1996**, *102*, 82−85. (i) Daniel, C.; Menelle, A.; Brulet, A.; Guenet, J.-M. *Polymer* **1997**, *38*, 4193−4199. (j) Daniel, C.; Musto, P.; Guerra, G. *Macromolecules* **2002**, *35*, 2243−2251. (k) Daniel, C.; Alfano, D.; Guerra, G.; Musto, P. *Macromolecules* **2003**, *36*, 5742−5750. (l) Shimizu, H.; Wakayama, T.; Wada, R.; Okabe, M.; Tanaka, F. *Polym. J.* **2005**, *37*, 294−298.
(8) (a) Daniel, C.; Deluca, M. D.; Guenet, J. M.; Brulet, A.; Menelle, A. *Polymer* **1996**, *37*, 1273−1280. (b) Rastogi, S.; Goossens, J. G. P.; Lemstra, P. J. *Macromolecules* **1998**, *31*, 2983−2998. (c) Van Hooy-Corstjens, C. S. J.; Magusin, P. C. M.; Rastogi, S.; Lemstra, P. J. *Macromolecules* **2002**, *35*, 6630−6637. (d) Malik, S.; Rochas, C.; Guenet, J. M. *Macromolecules* **2006**, *39*, 1000−1007.
(9) Daniel, C.; Alfano, D.; Venditto, V.; Cardea, S.; Reverchon, E.; Larobina, D.; Mensitieri, G.; Guerra, G. *Adv. Mater.* **2005**, *17*, 1515−1518.
(10) Klug, H. P.; Alexander, L. E. In *X-ray Diffraction Procedure*; John Wiley: New York, 1959; Chapter 9.
(11) (a) Grulke, E. In *Polymer Handbook*, 3rd ed.; John Wiley: New York, 1989; Vol. VII, p 519. (b) Errede L. A. In *Molecular Interpretations of Sorption in Polymers, Part I*; Springer-Verlag: Berlin, 1991.
(12) Daniel, C.; Avallone, A.; Rizzo, P.; Guerra, G. *Macromolecules* **2006**, *39*, 4820−4823.
(13) (a) Al-Muhtaseb, S. A.; Ritter, J. A. *Adv. Mater.* **2003**, *15*, 101−114. (b) Cooper, A. I. *Adv. Mater.* **2003**, *15*, 1049−1058. (c) Valentin, R.; Molvinger, K.; Quignard, F.; Di Renzo, F. *Macromol. Symp.* **2005**, *222*, 93−101.
(14) (a) Malik, S.; Rochas, C.; Schmutz, M.; Guenet, J. M. *Macromolecules* **2005**, *38*, 6024−6030. (b) Itagaki, H.; Mochizuchi, J. *Macromolecules* **2005**, *38*, 9625−9630.
(15) (a) Rizzo, P.; Spatola, A; De Girolamo Del Mauro, A.; Guerra, G. *Macromolecules* **2005**, *38*, 10089−10094. (b) Rizzo, P.; Lamberti, M.; Albunia, A.; Ruiz de Ballesteros, O.; Guerra, G. *Macromolecules* **2002**, *35*, 5854−5860. (c) Rizzo, P.; Albunia, A. R.; Milano, G.; Venditto, V.; Guerra, G.; Mensitieri, G.; Di Maio, L. *Macromol. Symp.* **2002**, *185*, 65−75.
(16) (a) Milano, G.; Guerra, G.; Müller-Plathe, F. *Chem. Mater.* **2002**, *14*, 2977−2982. (b) Venditto, V.; De Girolamo Del Mauro, A.; Mensitieri, G.; Milano, G.; Musto, P.; Rizzo, P.; Guerra, G. *Chem. Mater.* **2006**, *18*, 2205−2210.

MA061124K